Journal of Applied Sciences

ISSN 1812-5654

science alert

ANSInet
an open access publisher
http://ansinet.com

Journal of Applied Sciences 10 (15): 1563-1571, 2010
ISSN 1812-5654

Power Flow Study Including FACTS Devices

[1]A.K. Sahoo, [2]S.S. Dash and [3]T. Thyagarajan
[1]Department of Electrical and Electronics Engineering,
SSN College of Engineering, OMR, Kalavakkam, TN-603 110, India
[2]Department of Electrical and Electronics Engineering,
SRM University, Katankulathur, Tamil Nadu, 603 203, India
[3]Department of Instrumentation Engineering, MIT, Anna University, Chennai, India

Abstract: The electric power industry is undergoing the most profound technical, economic and organizational changes since, its inception some one hundred years ago. This paradigm is the result of the liberalization process, stipulated by politics and followed up by industry. In countries like India with fast growing demand of electric power it is difficult to extend the transmission system in time by either building new lines or by introduction of a new voltage level. Power is therefore transmitted through weak system leading to unsatisfactory quality and reliability of power supply. So, the need for new power flow controllers capable of increasing transmission capacity and controlling power flows through predefined transmission corridors will certainly increase. For this reason, as well known in recent years a new class of controllers, Flexible AC Transmission System (FACTS) controllers have rapidly met with favor. Considering the practical application of the FACTS controller, it is of importance to investigate the benefits as well as model these devices for power system steady state operation. We have performed the comprehensive modeling of most popular FACTS devices for power flow study. The effectiveness of modeling and convergence is tested with a five bus study system without any FACTS devices and further analyzed it with different FACTS controllers. The de facto standard Newton-Raphson method is used to solve the nonlinear power flow equation. Also, the study is extended for IEEE 30 bus and IEEE 118 bus system. Programming of the power flow studies stated above is implemented with MATLAB.

Key words: FACTS controller, SVC, TCSC, STATCOM, UPFC

INTRODUCTION

The electricity supply industry is undergoing a profound transformation worldwide. Market forces, scarcer natural resources and an ever-increasing demand for electricity are some of the drivers responsible for such an unprecedented change. Against this background of rapid evolution, the expansion programmes of many utilities are being thwarted by a variety of well-founded, environmental, land use and regulatory pressures that prevent the licensing and building of new transmission lines and electricity generating units. An in-depth analysis of the options available for maximizing existing transmission assets, with high levels of reliability and stability, has pointed in the direction of power electronics. There is general agreement that novel power electronics equipment and techniques are potential substitutes for conventional solutions, which are normally based on electromechanical technologies that have slow response times and high maintenance costs (Hingorani and Gyugyi, 2000).

Until recently, active and reactive power control in AC transmission networks was exercised by carefully adjusting transmission line impedances, as well as regulating terminal voltages by generator excitation control and by transformer tap changes. At times, series and shunt impedances were employed to effectively change line impedances. The FACTS technology is most interesting for transmission planners because it opens up new opportunities for controlling power and enhancing the usable capacity of present, as well as new and upgraded, lines. The possibility that current through a line can be controlled at a reasonable cost enables a large potential of increasing the capacity of existing lines with large conductors and use of one of the FACTS controllers to enable corresponding power to flow through such lines under normal and contingency conditions (Hingorani, 1993; Mathur and Varma, 2002).

Corresponding Author: Ashwin Kumar Sahoo, Department of Electrical and Electronics Engineering, SSN College of Engineering, OMR, Kalavakkam, TN-603 110, India Tel/Fax: (+91)044-2747 4844/45/46

POWER FLOW ANALYSIS

Planning the operation of power systems under existing conditions, its improvement and also its future expansion require the load flow studies, short circuit studies and stability studies.

Through the load flow studies we can obtain the voltage magnitudes and angles at each bus in the steady state. This is rather important, as the magnitudes of the bus voltages are required to be held within a specified limit. Once the bus voltage magnitudes and their angles are computed using the load flow, the real and reactive power flow through each line can be computed. Also based on the difference between power flow in the sending and receiving ends, the losses in a particular line can also be computed. One of the main strengths of the Newton Raphson method is its reliability towards convergence. Contrary to non Newton Raphson solutions, convergence is independent of the size of the network being solved and the number and kinds of control equipment present in the system. So, this is the most favored power flow method (Acha *et al*., 2004; Fuerte-Esquivel and Acha, 1997).

The Newton Raphson algorithm: In large-scale power flow studies, the Newton raphson has proved most successful owing to its strong convergence characteristics. The power flow Newton Raphson algorithm is expressed by the following relationship (Milano, 2009; Bonert, 1998).

$$\begin{bmatrix}\Delta P\\ \Delta Q\end{bmatrix} = -\begin{bmatrix}\Delta P/\Delta\theta & \Delta P/(\Delta v/v)\\ \Delta Q/\Delta\theta & \Delta Q/(\Delta v/v)\end{bmatrix}\begin{bmatrix}\Delta\theta\\ (\Delta v/v)\end{bmatrix} \quad (1)$$

It may be pointed out that the correction terms ΔV_m are divided by V_m to compensate for the fact that jacobian terms $(\partial P_m/\partial V_m)V_m$ and $(\partial Q_m/\partial V_m)V_m$ are multiplied by V_m. It is shown in the directive terms that this artifice yields useful simplifying calculations. Consider the lst element connected between buses k and m in Fig. 1, for which self and mutual Jacobian terms are given below:

For k ≠ m.

$$\frac{\partial P_{k,1}}{\partial \theta_{m,1}} = V_k V_m[G_{km}\sin(\theta_k-\theta_m) - B_{km}\cos(\theta_k-\theta_m)] \quad (2)$$

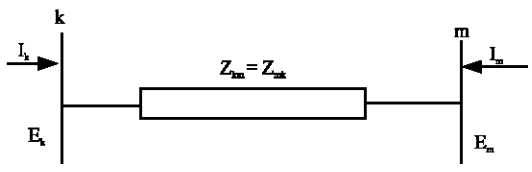

Fig. 1: Equivalent impedance

$$\frac{\partial P_{k,1}}{\partial V_{m,1}/V_{m,1}} = V_k V_m[G_{km}\cos(\theta_k-\theta_m) + B_{km}\sin(\theta_k-\theta_m)] \quad (3)$$

$$\frac{\partial Q_{k,1}}{\partial \theta_{m,1}} = -\frac{\partial P_{k,1}}{\partial V_{m,1}/V_{m,1}} \quad (4)$$

$$\frac{\partial Q_{k,1}}{\partial V_{m,1}/V_{m,1}} = \frac{\partial P_{k,1}}{\partial \theta_{m,1}} \quad (5)$$

For k = m:

$$\frac{\partial P_{k,1}}{\partial \theta_{k,1}} = -Q_k^{cal} - V_k^2 B_{kk} \quad (6)$$

$$\frac{\partial P_{k,1}}{\partial V_{k,1}/V_{k,1}} = P_k^{cal} + V_k^2 G_{kk} \quad (7)$$

$$\frac{\partial Q_{k,1}}{\partial \theta_{k,1}} = P_k^{cal} - V_k^2 G_{kk} \quad (8)$$

$$\frac{\partial Q_{k,1}}{\partial V_{k,1}/V_{k,1}} = Q_k^{cal} - V_k^2 B_{kk} \quad (9)$$

The mutual elements remain the same whether we have one transmission line or n transmission lines terminating at the bus k.

The sample 5 bus system: In case study we have considered the five bus system as shown in Fig. 2. The input data for the considered system are shown in Table 1 for the bus and Table 2 for transmission line. Assuming base quantities of 100 MVA and 100 KV. The result for the above system is shown in Table 3. All the nodal voltages are achieved to be within acceptable voltage magnitude limits.

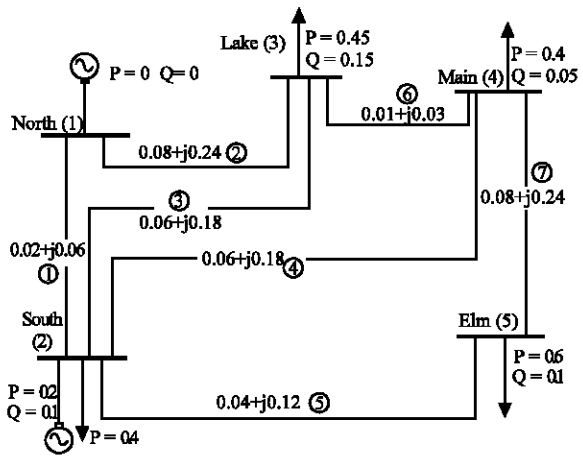

Fig. 2: The five-bus network

Table 1: Input bus data for the study system (p.u.)

		Generation		Load		Voltage	
Bus No.	Type	P	Q	P	Q	|v|	Ø
1	slack	0	0	-	-	1	0
2	P-V	0	0	0.2	0.10	1	0
3	P-Q	-	-	0	0.15	1	0
4	P-Q	-	-	0	0.05	1	0
5	P-Q	-	-	1	0.10	1	0

Table 2: Input transmission line data for the study system (p.u.)

Bus No.	Bus code (k-m)	Impedance (R+jX)	Line charging admittance
1	1-2	0.02+j0.06	0+j0.06
2	1-3	0.08+j0.24	0+j0.05
3	2-3	0.06+j0.18	0+j0.04
4	2-4	0.06+j0.18	0+j0.04
5	2-5	0.04+j0.12	0+j0.03
6	3-4	0.01+j0.03	0+j0.02
7	4-5	0.08+j0.24	0+j0.05

Table 3: Power flow result of study system without any FACTS devices

Parameters	Bus 1	Bus 2	Bus 3	Bus 4	Bus 5
VM (p.u)	1.06	1.00	0.987	0.984	0.972
VA (deg)	0.00	-2.06	-4.640	-4.96	-5.770

POWER FLOW MODEL OF FACTS DEVICES

Power flow model of SVC

Shunt variable susceptance model: In practice the SVC can be seen as an adjustable reactance with either firing angle limits or reactance limits. The equivalent circuit shown in Fig. 3 is used to derive the SVC nonlinear power equations and the liberalized equations required by the Newton's method (Bijwe and Kelapure, 2003). With reference to Fig. 3, the current drawn by the SVC is $I_{SVC}=jB_{SVC}V_k$ and the reactive power drawn by the SVC, which is also the reactive power injected at bus k, is $Q_{SVC} = Q_k = -V_k^2B_{SVC}$. At the end of each iteration, the variable Shunt Susceptance B is updated according to:

$$B_{SVC}^{(i)} = B_{SVC}^{(i-1)} + \left(\frac{\Delta B_{SVC}}{B_{SVC}}\right)^{(i)} B_{SVC}^{(i-1)} \quad (10)$$

The changing Susceptance represents the total SVC Susceptance necessary to maintain the nodal voltages at specified value.

Firing angle model: An alternative SVC model, which circumvents the additional iterative process, consists in handling the thyristor controlled reactor (TCR) firing angle α as a state variable in the power flow formulation. The positive sequence Susceptance of the SVC, is given by:

$$Q_k = \frac{-V_k^2}{X_C X_L}\{X_L - \frac{X_C}{\pi}[2(\pi - \alpha_{SVC}) + \sin(2\alpha_{SVC})]\} \quad (11)$$

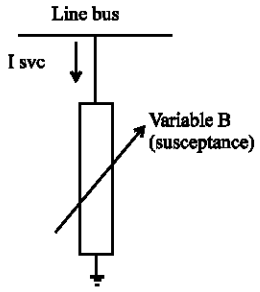

Fig. 3: Variable shunt susceptance

From the above equation, the linearised SVC equation is given as:

$$\begin{bmatrix}\Delta P_k\\ \Delta Q_k\end{bmatrix}(i) = \begin{bmatrix}0 & 0\\ 0 & \frac{2V^2}{\pi X_L}[\cos(2\alpha_{SVC})-1]\end{bmatrix}(i)\begin{bmatrix}\Delta\theta_k\\ \Delta\alpha_{SVC}\end{bmatrix}(i) \quad (12)$$

At the end of iteration (i), the variable firing angle α_{SVC} is updated according to $\alpha_{SVC}^{(i)} = \alpha_{SVC}^{(i-1)} + \Delta\alpha_{SVC}^{(i)}$

Power flow model of TCSC: Two alternative power flow models to assess the impact of TCSC equipment in network wide applications are presented here. The simpler TCSC model exploits the concept of a variable series reactance. The series reactance is adjusted automatically, within limits, to satisfy a specified amount of active power flows through it. The more advanced model uses directly the TCSC reactance-firing angle characteristics, given in the form of a non- linear relation. The TCSC firing angle is chosen to be the state variable in the Newton-Raphson power flow solution.

Variable series impedance power flow model: The TCSC power flow model presented in this section is based on the simple concept of a variable series reactance, the value of which is adjusted automatically to constrain the power flow across the branch to a specified value. Nelson *et al.* (1995). The amount of reactance is determined efficiently using Newton's method. The changing reactance $X_{TCSC,}$ shown in Fig. 4, represents the equivalent reactance of all the series-connected modules making up the TCSC, when operating either in inductive or in the capacitive regions. The transfer admittance matrix of the variable series compensator shown in Fig. 4 is given by:

$$\begin{bmatrix}I_k\\ I_m\end{bmatrix} = \begin{bmatrix}jB_{kk} & jB_{km}\\ jB_{mk} & jB_{mm}\end{bmatrix}\begin{bmatrix}V_k\\ V_m\end{bmatrix} \quad (13)$$

For inductive operation, we have:

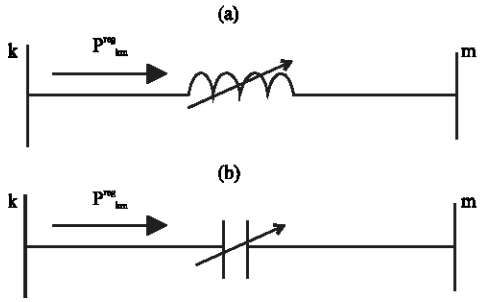

Fig. 4: Thyristor controlled series compensator equivalent circuit, (a) Inductive and (b) capacitive operative regions

$$B_{kk} = B_{mm} = -\frac{1}{X_{TCSC}}$$

$$B_{km} = B_{mk} = \frac{1}{X_{TCSC}} \quad (14)$$

For capacitive operation the signs are reversed. The active and reactive power equations at bus k are:

$$P_k = V_k V_m B_{km} \sin(\theta_k - \theta_m) \quad (15)$$

$$Q_k = -V_k^2 B_{kk} - V_k V_m B_{km} \cos(\theta_k - \theta_m) \quad (16)$$

For the power equations at bus m, the subscripts k and m are exchanged in the above equations. The state variable X_{TCSC} of the series controller is updated at the end of each iterative step according to:

$$X_{TCSC}^{(i)} = X_{TCSC}^{(i-1)} + \left(\frac{\Delta X_{TCSC}}{X_{TCSC}}\right)^{(i)} X_{TCSC}^{(i-1)} \quad (17)$$

Firing angle power flow model: The model presented in this section uses the concept of an equivalent series reactance to represent the TCSC. Once the value of reactance is determined using Newton's method then the associated firing angle α_{TCSC} can be calculated. However, such calculations involve an iterative solution since the TCSC reactance and the firing angle are nonlinearly related. One way to avoid the additional iterative process is to use the alternative TCSC power flow model presented in this section. The fundamental frequency equivalent reactance X_{TCSC} of the TCSC module shown in Fig. 5 is:

$$X_{TCSC} = -X_C + C_1\{2(\pi-\alpha) + \sin[2(\pi-\alpha)]\} - C_2\cos^2(\pi-\alpha)\{\omega\tan[\omega(\pi-\alpha)] - \tan(\pi-\alpha)\} \quad (18)$$

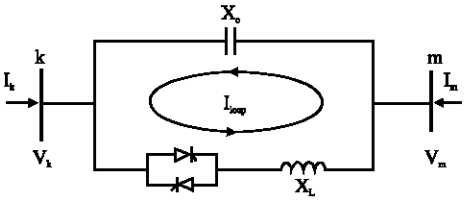

Fig. 5: Thyristor controlled series compensator firing angle module

where:

$$C_1 = \frac{X_C + X_{LC}}{\pi}$$

$$C_2 = \frac{4X_{LC}^2}{X_L \pi}$$

$$X_{LC} = \frac{X_C X_L}{X_C - X_L}$$

$$\omega = \left(\frac{X_C}{X_L}\right)^{1/2}$$

The TCSC active and reactive power equations at bus k are:

$$P_k = V_k V_m B_{km} \sin(\theta_k - \theta_m) \quad (19)$$

$$Q_k = -V_k^2 B_{kk} - V_k V_m B_{km} \sin(\theta_k - \theta_m) \quad (20)$$

where, $B_{kk} = -B_{km} = B_{TCSC}$.

Power flow model of static synchronous compensator: The Static Synchronous Compensator (STATCOM) is represented by a synchronous voltage source with minimum and maximum voltage magnitude limits. The bus at which STATCOM is connected is represented as a PV bus, which may change to a PQ bus in the events of limits being violated. In such case, the generated or absorbed reactive power would correspond to the violated limit. The power flow equations for the STATCOM are derived below from the first principles and assuming the following voltage source representation (Gyugi, 1994).

Based on the shunt connection shown in Fig. 6, the following equation may be written:

$$E_{vR} = V_{vR}(\cos\delta_{vR} + j\sin\delta_{vR}) \quad (21)$$

$$S_{vR} = V_{vR} I_{vR}^* = V_{vR} Y_{vR}^* (V_{vR}^* - V_k^*) \quad (22)$$

where, * represents the complex conjugate.

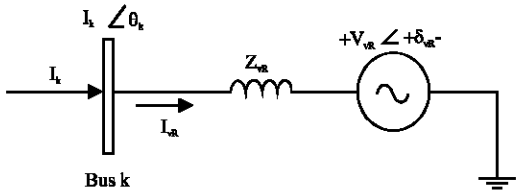

Fig. 6: Static compensator (STATCOM) equivalent circuits

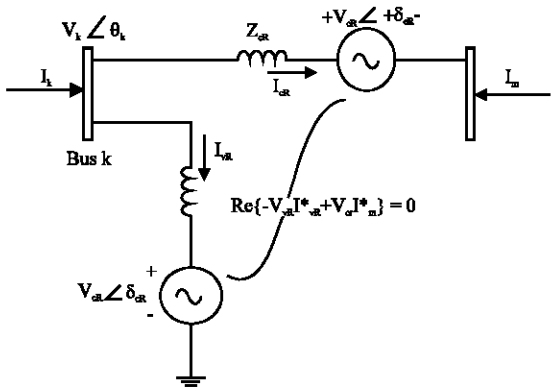

Fig. 7: Unified power flow controller equivalent circuit

The following are the active and reactive power equations for the converter at bus k,

$$P_{vR} = V_{vR}^2 G_{vR} + V_{vR} V_k [G_{vR} \cos(\delta_{vR} - \theta_k) + B_{vR} \sin(\delta_{vR} - \theta_k)]$$

$$Q_{vR} = -V_{vR}^2 B_{vR} + V_{vR} V_k [G_{vR} \sin(\delta_{vR} - \theta_k) - B_{vR} \cos(\delta_{vR} - \theta_k)]$$

$$P_k = V_k^2 G_{vR} + V_k V_{vR} [G_{vR} \cos(\theta_k - \delta_{vR}) + B_{vR} \sin(\theta_k - \delta_{vR})]$$

$$Q_k = -V_k^2 B_{vR} + V_k V_{vR} [G_{vR} \sin(\theta_k - \delta_{vR}) - B_{vR} \cos(\theta_k - \delta_{vR})]$$

Power flow model of unified power flow controller: The UPFC equivalent circuit consists of two coordinated synchronous voltage sources for the purpose of fundamental frequency steady state analysis. Such an equivalent circuit is shown in Fig. 7.

The UPFC voltage sources are:

$$E_{vR} = V_{vR} (\cos\delta_{vR} + j\sin\delta_{vR}) \quad (23)$$

$$E_{cR} = V_{cR} (\cos\delta_{cR} + j\sin\delta_{cR}) \quad (24)$$

where, V_{vR} and δ_{vR} are the controllable magnitude ($V_{vRmin} \le V_{vR} \le V_{vRmax}$) and phase angle ($0 \le \delta_{vR} \le \delta 2\pi$) of the voltage source representing the shunt converter. The magnitude V_{cR} and phase angle δ_{cR} of the voltage source representing the series converter are controlled between limits ($V_{cRmin} \le V_{cR} \le V_{cRmax}$) and ($0 \le \delta_{cR} \le 2\pi$), respectively. The phase angle of the series injected voltage determines the mode of power flow control (Kannan *et al*., 2004; Gyugyi *et al*., 1995). If δ_{cR} is in phase with the nodal voltage angle $\ominus_k$, the UPFC regulates the terminal voltage. If δ_{cR} is in quadrature with $\ominus_k$, it controls active power flow, acting as a phase shifter. If δ_{cR} is in quadrature with line current angle then it controls active power flow, acting as a variable series compensator. At any other value of δ_{cR}, the UPFC operates as a combination of voltage regulator, variable series compensator and phase shifter. The magnitude of the series injected voltage determines the amount of power flow to be controlled. Based on the equivalent circuit shown in Fig. 7 the active and reactive power equations are:

At bus k:

$$\begin{aligned} P_k &= V_k^2 G_{kk} + V_k V_m [G_{km} \cos(\theta_k - \theta_m) + B_{km} \sin(\theta_k - \theta_m)] \\ &+ V_k V_{cR} [G_{km} \cos(\theta_k - \delta_{cR}) + B_{km} \sin(\theta_k - \delta_{cR})] \\ &+ V_k V_{vR} [G_{vR} \cos(\theta_k - \delta_{vR}) + B_{vR} \sin(\theta_k - \delta_{vR})] \end{aligned} \quad (25)$$

$$\begin{aligned} Q_k &= -V_k^2 B_{kk} + V_k V_m [G_{km} \sin(\theta_k - \theta_m) - B_{km} \cos(\theta_k - \theta_m)] \\ &+ V_k V_{cR} [G_{km} \sin(\theta_k - \delta_{cR}) - B_{km} \cos(\theta_k - \delta_{cR})] \\ &+ V_k V_{vR} [G_{vR} \sin(\theta_k - \delta_{vR}) - B_{vR} \cos(\theta_k - \delta_{vR})] \end{aligned} \quad (26)$$

At bus m:

$$\begin{aligned} P_m &= V_m^2 G_{mm} + V_m V_k [G_{mk} \cos(\theta_m - \theta_k) + B_{mk} \sin(\theta_m - \theta_k)] \\ &+ V_m V_{cR} [G_{mm} \cos(\theta_m - \delta_{cR}) + B_{mm} \sin(\theta_m - \delta_{cR})] \end{aligned} \quad (27)$$

$$\begin{aligned} Q_m &= -V_m^2 B_{mm} + V_m V_k [G_{mk} \sin(\theta_m - \theta_k) - B_{mk} \cos(\theta_m - \theta_k)] \\ &+ V_m V_{cR} [G_{mm} \sin(\theta_m - \delta_{cR}) - B_{mm} \cos(\theta_m - \delta_{cR})] \end{aligned} \quad (28)$$

Series converter:

$$\begin{aligned} P_{cR} &= V_{cR}^2 G_{mm} + V_{cR} V_k [G_{km} \cos(\delta_{cR} - \theta_k) + B_{km} \sin(\delta_{cR} - \theta_k)] \\ &+ V_{cR} V_m [G_{mm} \cos(\delta_{cR} - \theta_m) + B_{mm} \sin(\delta_{cR} - \theta_m)] \end{aligned} \quad (29)$$

$$\begin{aligned} Q_{cR} &= -V_{cR}^2 B_{mm} + V_{cR} V_k [G_{km} \sin(\delta_{cR} - \theta_k) - B_{km} \cos(\delta_{cR} - \theta_k)] \\ &+ V_{cR} V_m [G_{mm} \sin(\delta_{cR} - \theta_m) - B_{mm} \cos(\delta_{cR} - \theta_m)] \end{aligned} \quad (30)$$

Shunt converter:

$$P_{vR} = -V_{vR}^2 G_{vR} + V_{vR} V_k [G_{vR} \cos(\delta_{vR} - \theta_k) + B_{vR} \sin(\delta_{vR} - \theta_k)] \quad (31)$$

$$Q_{vR} = V_{vR}^2 B_{vR} + V_{vR} V_k [G_{vR} \sin(\delta_{vR} - \theta_k) - B_{vR} \cos(\delta_{vR} - \theta_k)] \quad (32)$$

Assuming lossless converter values, the active power supplied to the shunt converter, P_{vR}, equals the active power demanded by the series converter, P_{cR}, i.e., $P_{vR}+P_{cR} = 0$. Further more, if the coupling transformers are assumed to contain no resistance then the active power at bus k matches the active power at bus m. Accordingly, $P_{vR}+P_{cR} = P_k+P_m = 0$. The UPFC power equations are combined with those of the AC network.

CASE STUDIES WITH FACTS CONTROLLERS

Power flow study with SVC: The SVC is included in the bus 3 (Fig. 8) of the sample system to maintain the nodal voltage at 1 p.u.

The SVC data:

- The initial susceptance: 0.02 p.u

For the firing angle model:

- The initial firing angle:140 degrees
- Inductive reactance: 0.288 p.u
- Capacitive reactance: 1.07 p.u

The result for the voltage magnitude and phase angle obtained for the above system for both variable Susceptance and Firing angle model is shown in Table 4. Due to the inclusion of SVC in the third bus, its voltage is maintained at 1 p.u.

Power flow study with TCSC: The original five-bus network is modified to include one TCSC (Fig. 9) to compensate the transmission line connected between bus 3 and 4. The TCSC should maintain the real power flow in transmission line 6 as 21 MW.

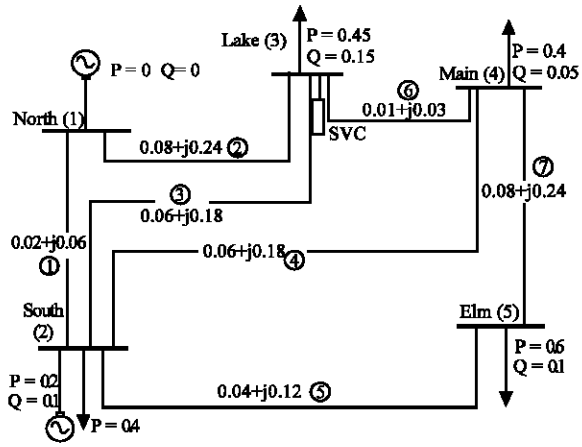

Fig. 8: Study System with SVC included

TCSC data:

- Initial capacitive reactance: 0.015 p.u.

In the firing angle model:

- Firing angle:145 degrees

The result for the voltage magnitude and phase angle obtained for the above system for both variable reactance and firing angle model is shown in Table 5. Due to the inclusion of TCSC, the target power flow of 21 MW in line 6 is maintained.

Power flow study with statcom: The STATCOM is included in the bus 3 (Fig. 10) of the sample system to maintain the nodal voltage at 1 p.u.

Statcom data:

- The initial source voltage magnitude: 1 p.u.
- Phase angle: 0 degrees.
- The converter reactance: 10 p.u.

The power flow result indicates that the STATCOM generates 20.5 MVar in order to keep the voltage magnitude at 1 p.u. at bus3. Use of STATCOM results in an improved network voltage profile as shown in Table 6.

Table 4: Result with SVC included in Bus 3

Parameters	Bus 1	Bus 2	Bus 3	Bus 4	Bus 5
VM (p.u)	1.06	1	1	0.9944	0.9752
VA (deg)	0.00	-2.0532	-4.8378	-5.1071	-5.7972

Table 5: Result with TCSC included in line 6

Parameters	Bus 1	Bus 2	Bus 3	Bus 4	Bus 5
VM (p.u)	1.1	1	0.9869	0.9846	0.9719
VA (deg)	0	-2.0378	-4.7239	-4.8145	-5.7012

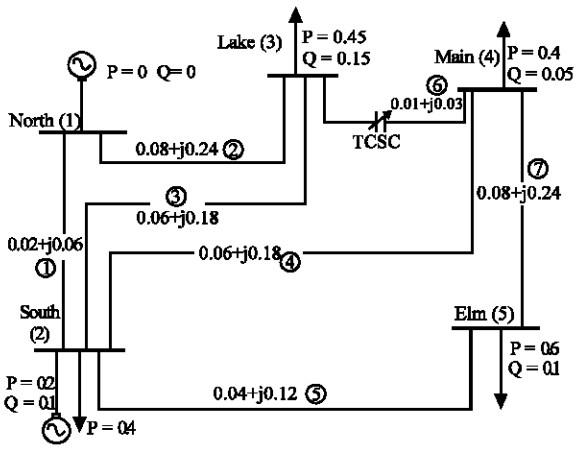

Fig. 9: Study System with TCSC included

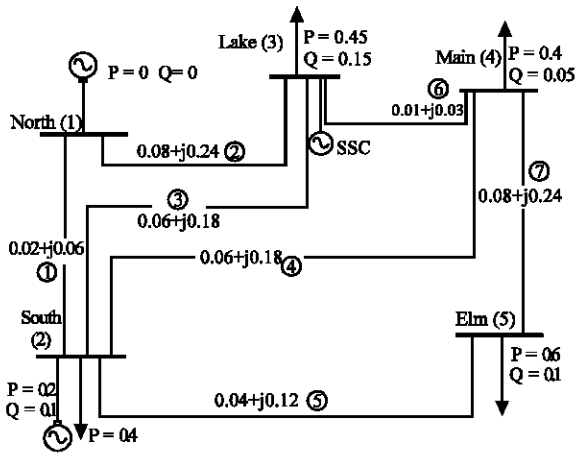

Fig. 10: Study System with STATCOM included

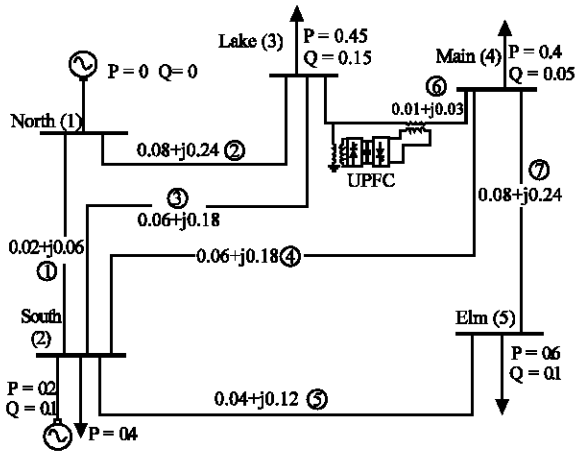

Fig. 11: Study System with UPFC included

Table 6: Result with STATCOM included in Bus 3

Parameters	Bus 1	Bus 2	Bus 3	Bus 4	Bus 5
VM (p.u)	1.1	1	1	0.9944	0.9752
VA (deg)	0	-2.04	-4.7526	-4.821	-5.8259

Table 7: Result with UPFC included in line 6

Parameters	Bus 1	Bus 2	Bus 3	Bus 4	Bus 5
VM (p.u)	1.1	1	1	0.9917	0.9745
VA (deg)	0	-1.7691	-6.061	-3.1905	-4.9737

Power flow study with UPFC: The original five-bus network is modified to include one UPFC to compensate the transmission line linking bus 3 and bus 4 (Fig. 11). UPFC should maintain real and reactive power flowing towards bus 4 at 40 MW and 2 MVar, respectively. The UPFC shunt converter is set to regulate the nodal voltage magnitude at bus 3 at 1 p.u. as shown in Table 7.

UPFC data: The starting values of the UPFC shunt converter are:

- Voltage magnitude: 1 p.u.
- Phase angle: 0 degrees
- For series converter:
- Voltage magnitude: 0.04 p.u.
- Phase angle: 87.13 degrees
- Reactance for both the converters: 0.1 p.u.

RESULTS

The power flow for the five bus system was analyzed without and with FACTS devices performing the Newton-Raphson method. The largest power flow takes place in the transmission line connecting the two generator buses: 89.3 MW and 74.02 MVar leave bus1and 86.8 MW and 72.9 MVar arrive at bus2. The operating conditions demand a large amount of reactive power generation by the generator connected at bus1 (i.e., 90.82 MVar). This amount is well in excess of the reactive power drawn by the system loads (i.e., 40 MVar). The generator at bus2 draws the excess of reactive power in the network (i.e., 61.59 MVar). This amount includes the net reactive power produced by several transmission lines, which is addressed by different FACTS devices. Thus SVC upholds its target value and as expected identical power flows and bus voltages are obtained for both Shunt Variable Susceptance Model and Firing angle power flow models.

The TCSC variable series compensator model is used to maintain active power flowing from the extra fictious bus 6 towards bus 3 at 21 MW. The starting value of the TCSC is set at 50% of the value of transmission line inductive reactance. The TCSC upholds the target value of 21 MW, which is achieved with 70% series compensation of the transmission line 6. In the case of the firing angle model the initial value of firing angle is set at 145° and the TCSC upholds the target value of 21 MW.

The power flow result indicates that the STATCOM generates 20.5 MVar in order to keep the voltage magnitude at 1 p.u., at bus 3. Use of STATCOM results in an improved network voltage profile, except at bus 5, which is too far away from bus 3 to benefit from the influence of STATCOM.

The original five-bus network is modified to include one UPFC to compensate the transmission line linking bus 3 and bus 4 The UPFC is used to maintain active and reactive powers leaving UPFC, towards bus 4, at 40 MW and 2 MVar, respectively. Moreover, the UPFC shunt converter is set to regulate the nodal voltage magnitude at bus 3 at 1 p.u. There is a 32% increase of active power flowing towards bus3. The increase is in response to the large amount of active power demanded by the UPFC series converter. Thus from the above analysis we find

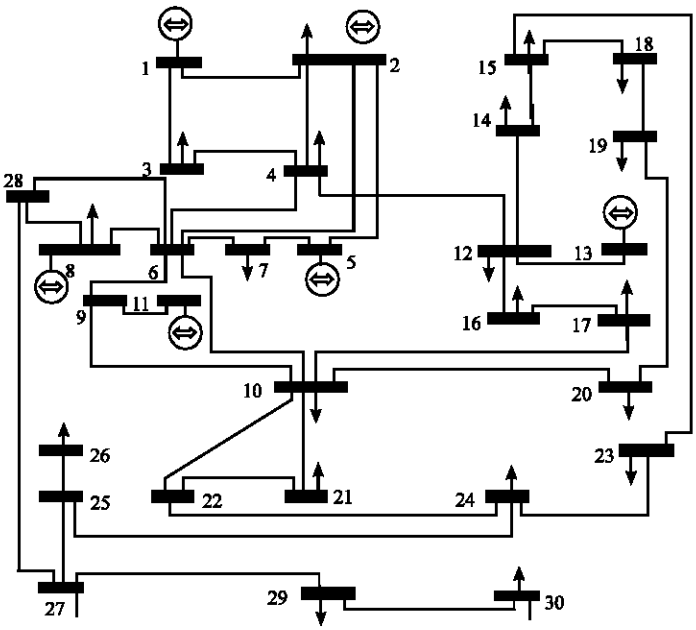

Fig. 12: Single line circuit diagram of the IEEE 30-bus system

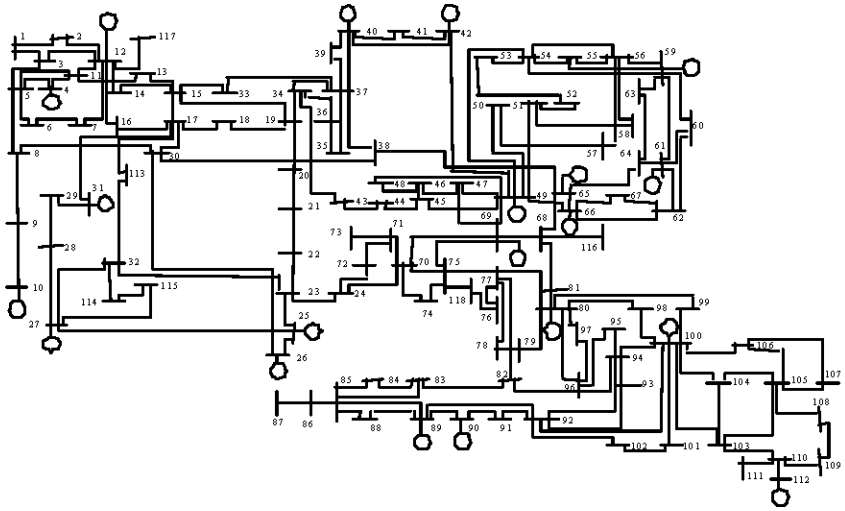

Fig. 13: Single line circuit diagram of the IEEE 118-bus system

that within the framework of traditional power transmission concepts, the UPFC is able to control, simultaneously or selectively, all the parameters affecting power flow in the transmission line (voltage, impedance and phase angle) and this unique capability is signified by the adjective unified in its name.

To verify the proposed different FACTS steady state model, numerical studies have been carried out on the IEEE 30-bus system (Fig. 12) and IEEE 118-bus system (Fig. 13). In the tests, a convergence of 1.0e-12 p.u., is used for maximal absolute bus power mismatch. The convergence of result is achieved within 4 to 5 iterations.

CONCLUSION

The model developed for different FACTS devices are used in the 5 bus, IEEE 30 bus and IEEE 118 bus system to perform power flow solutions. The effectiveness of the models developed is reflected in quick convergence during the power flow study.

ACKNOWLEDGMENT

The authors are thankful to the management of SSN College of Engineering, Kalavakkam, Chennai for providing the Computational facilities to carryout this study.

REFERENCES

Acha, E., C.R. Fuerte-Esquivel, H. Ambriz-Perez and C. Angeles-Camacho, 2004. FACTS: Modeling and Simulation in Power Networks. 1st Edn., John Wiley and Sons Inc., New York, ISBN: 978-0470852712.

Bijwe, P.R. and S.M. Kelapure, 2003. Nondivergent fast power flow methods. IEEE Trans. Power Syst., 18: 633-638.

Bonert, R., 1998. A laboratory for power systems control with static converters. IEEE Trans. Power Syst., 13: 15-20.

Fuerte-Esquivel, C.R. and E. Acha, 1997. A Newton-type algorithm for the control of power flow in electrical power networks. IEEE Trans. Power Syst., 12: 1474-1480.

Gyugi, L., 1994. Dynamic compensation of AC transmission lines by solid state synchronous voltage sources. IEEE Tran. Power Delivery, 9: 904-911.

Gyugyi, L., C.D. Schauder, S.L. Williams, T.R. Rietman, D.R. Torgerson and A. Edris, 1995. The unified power flow controller: A new approach to power transmission control. IEEE Trans. Power Delivery, 10: 1085-1097.

Hingorani, N.G. and L. Gyugyi, 2000. Understanding FACTS: Concept and Technology of Flexible AC Transmission System. IEEE Press, Piscataway, NJ.

Hingorani, N.G., 1993. Flexible AC transmission. IEEE Spectrum, 30: 40-45.

Kannan, S., S. Jayaram and M.M.A. Salama, 2004. Real and reactive power coordination for a unified power flow controller. IEEE Trans. Power Syst., 19: 1454-1461.

Mathur, R.M. and R.K. Varma, 2002. Thyristor-based FACTS Controllers for Electrical Transmission Systems. 1st Edn., Wiley-Interscience, New York, USA., ISBN: 978-0-471-20643-9, pp: 495.

Milano, F., 2009. Continuous Newton's method for power flow analysis. IEEE Trans. Power Syst., 24: 50-57.

Nelson, R.J., J. Bian and S.L. Willliams, 1995. Transmission series power flow control. IEEE Trans. Power Delivery, 10: 504-510.